Screening and classifying small molecule inhibitors of amyloid formation using ion mobility spectrometry-mass spectrometry

Lydia M. Young[1,2#], Janet C. Saunders[1,2#], Rachel A. Mahood[1,2], Charlotte H. Revill[1,3], Richard J. Foster[1,3], Ling-Hsien Tu[4], Daniel P. Raleigh[4], Sheena E. Radford[1,2]*, Alison E. Ashcroft[1,2]*

1. Astbury Centre for Structural Molecular Biology, University of Leeds, LS2 9JT, UK;
2. School of Molecular and Cellular Biology, University of Leeds, LS2 9JT, UK;
3. School of Chemistry, University of Leeds, LS2 9JT, UK;
4. Department of Chemistry, Stony Brook University, Stony Brook, NY 11794-3400, USA.

# These authors contributed equally to this work.

***** Corresponding authors:

email: **s.e.radford@leeds.ac.uk** and **a.e.ashcroft@leeds.ac.uk**

Abstract

The search for therapeutic agents which bind specifically to precursor protein conformations and inhibit amyloid assembly is an important challenge. Identifying such inhibitors is difficult since many protein precursors of aggregation are partially folded or intrinsically disordered, ruling out structure-based design. Furthermore, inhibitors can act by a variety of mechanisms, including specific or non-specific binding, as well as colloidal inhibition. Here we report a high throughput method based on ion mobility spectrometry-mass spectrometry (IMS-MS) that is capable of rapidly detecting small molecules that bind to amyloid precursors, identifying the interacting protein species, and defining the mode of inhibition. Using this method we have classified a variety of small molecules that are potential inhibitors of human islet amyloid polypeptide (hIAPP) aggregation or amyloid-beta 1-40 (Aβ40) aggregation as either specific, non-specific, colloidal or non-interacting. We also demonstrate the ability of IMS-MS to screen for inhibitory small molecules in a 96-well plate format and use this to discover a new inhibitor of hIAPP amyloid assembly.

Main Text

Aberrant aggregation of proteins and peptides into amyloid fibrils contributes to more than 50 human disorders, including Alzheimer's disease and type-2 diabetes mellitus[1]. The ability to screen for compounds able to disrupt protein aggregation, and assess their mode of action, is instrumental in therapy discovery. For folded proteins, structure-based design has been used to create small molecules able to stabilize the native state, thereby preventing the conformational changes required for protein aggregation to occur[2-4]. For aggregation-prone proteins that lack defined structure, discovery of small molecule inhibitors of aggregation is limited to screening using relatively low resolution approaches such as dye binding assays. Most biophysical techniques lack the sensitivity and resolution to detect and individually characterize oligomers during aggregation and, therefore, are not suitable for characterizing unique protein subspecies with which the small molecule inhibitor interacts[5]. Dye binding assays can also be compromised by competitive binding of the small molecule to the dye-binding site on the protein and by inner filter effects which can interfere with the fluorescence of the dye[6-8].

Electrospray ionization-ion mobility spectrometry-mass spectrometry (ESI-IMS-MS) circumvents the disadvantages of other *in vitro* screening techniques, allowing the rapid identification of inhibitors, the characterization of their mechanism of action, and the identification of the individual species to which the small molecule binds[9-11]. Here, we demonstrate the capability of ESI-IMS-MS to screen for, and analyze, the mode of interaction of a range of small molecules with human islet amyloid polypeptide (hIAPP, also known as amylin), a peptide associated with β-cell death in type-2 diabetes mellitus[12] and the failure of islet transplants, and amyloid beta 1-40 (Aβ40)[13], a peptide associated with Alzheimer's disease. ESI-IMS-MS has a number of additional benefits: it is rapid (<1 minute/sample), consumes low amounts of sample (~1000 molecules screened/mg protein), does not require sample labeling or immobilization, and provides stoichiometric and conformer-specific information. Additionally, colloidal inhibitors (that self-aggregate and

physically sequester proteins non-specifically[14]), that may erroneously be classified as “hits” in other assays, are immediately identifiable. While several small molecules have been shown to inhibit the fibrillation of hIAPP and/or Aβ40 *in vitro*[10,15-20], their mechanisms of action remain poorly understood. Using a selection of small molecules (Supplementary, Section 1 and Table S1), we demonstrate the ability of ESI-IMS-MS to differentiate and classify compounds that do not bind, and those that bind specifically, non-specifically or colloidally, to hIAPP and Aβ40 (Figure 1). Furthermore, we use the method developed to screen a further thirty compounds to demonstrate that it can be implemented in a high throughput mode and, in doing so, reveal a new specific inhibitor of hIAPP aggregation.

Results and Discussion

hIAPP forms oligomeric assemblies and fibrils in absence of inhibitor

The ESI mass spectrum of hIAPP (Figure 2a) shows predominantly monomer-related ions (e.g. 1^{2+} and 1^{3+}) together with traces of dimer and trimer (Figure 2b). hIAPP aggregates during fibril assembly forming oligomers dimer through to hexamer early in assembly which are readily observed using ESI-IMS-MS[10] (Figure 2c). The higher order oligomers appear and subsequently disappear as aggregation proceeds, resulting in the formation of long straight amyloid fibrils[10] (Figure 2b, inset).

ESI-IMS-MS-based screening approach

To determine the mode of action of different small molecules in inhibiting hIAPP self-assembly, 10 compounds were evaluated initially (Figure 1e). These were chosen because they, or their analogues, have been shown previously to inhibit, or have no observed effect, on amyloid formation (Supplementary, Section 1). Molar ratios of small molecule:hIAPP of 1:1 and 10:1 were used. The monomer and oligomer populations in the presence of each small molecule were characterized using ESI-IMS-MS. This technique has been implemented successfully to determine and rank ligand binding affinities[22-24]. However, ESI-MS can suffer from the drawback that hydrophobic interactions are not wholly maintained in the gas-phase which can lead to underestimates of binding affinity and/or false negative results. For this reason, fibril formation was also monitored using thioflavin T (ThT) fluorescence and the morphologies of the resulting aggregates were assessed using negative stain transmission electron microscopy (TEM). The objectives were to (i) observe interactions between peptide monomers or oligomers and each small molecule; (ii) determine how these interactions affect the distribution of monomeric conformers and oligomers; and (iii) elucidate whether any changes observed can be correlated with the inhibition (or lack of inhibition) of hIAPP amyloid formation.

Mode of action of a positive inhibitor of hIAPP fibril assembly

Using the ESI-IMS-MS-based screening approach described, the 10 compounds selected based on their known effect on hIAPP aggregation (Supplementary, Section 1 & Table S1) were analyzed. One of these was Fast Green FCF (**1**) (FG), a known inhibitor of hIAPP fibril formation[25].

Consistent with previous reports[25], ThT fluorescence and TEM (Figure 3a,b) confirmed that FG inhibits amyloid formation by hIAPP *in vitro*. However, the mechanism by which it inhibits assembly was unknown. Here, using ESI-IMS-MS, FG was found to bind to the 2+ and 3+ monomeric charge states of hIAPP (Figure 3c). Our previous work[10], and that of others[26], has shown that each hIAPP monomeric charge state (2+ and 3+) populates at least two conformers (extended and compact, with the more expanded structure proposed to be amyloid-prone). Analysis of the ESI-IMS-MS data reveals that FG alters the distribution of charge states and the monomeric conformers present, increasing the relative abundance of the 3+ monomer ion (Figure 3c) and the proportion of compact conformers compared with those observed for hIAPP alone (Supplementary, Figure S1). The interaction of FG likely involves the sulfonated groups forming favorable electrostatic interactions with positively charged hIAPP at pH 6.8 (hIAPP pI $\simeq$ 8.9). Consistent with this, the extent of binding is dependent on the buffer ionic strength (Supplementary, Figure S2). Factors other than electrostatic complementarity must contribute to the specific binding of FG, however, as not all sulfonated small molecules are inhibitors of hIAPP amyloid assembly (Supplementary, Section 1 & Figure S3). For two other known positive inhibitors, EGCG (epigallocatechin gallate)[10,16] (**2**) and silibinin[10,27] (**3**), low levels of binding are observed, despite complete inhibition of fibrillation, indicative of hydrophobic interactions playing a role in the binding interface. Unlike the hIAPP-FG interaction, this mode of binding is relatively insensitive to buffer ionic strength (Supplementary, Figure S2).

Colloidal inhibition characterized using ESI-IMS-MS

Congo red (CR) (**4**), was analysed as an example of a known colloidal inhibitor of hIAPP assembly[28]. At a 1:1 molar ratio of hIAPP:CR, a small increase in the rate of fibril formation was observed, with no significant change in the hIAPP mass spectrum (Figure 4a-c). However, at a 10:1 molar ratio of CR:hIAPP, no fibrillation was observed (Figure 4a,b). These data are consistent with previous reports that CR promotes fibril formation in some systems at low concentrations[29] but inhibits protein self-assembly when present at high concentrations (100-200 μM)[14]. Using ESI-IMS-MS, CR alone is observed to self-associate at high concentrations (320 μM), with aggregates ranging in size from ~5-11 copies (Supplementary, Figure S4). No binding of CR monomer to monomeric hIAPP was observed (Figure 4c), consistent with colloidal inhibition resulting from supramolecular assemblies of CR inhibiting fibril formation at high ligand concentrations.

Non-specific binding and lack of inhibition characterized using ESI-IMS-MS

Although not reported as an inhibitor of hIAPP aggregation, 1*H*-benzimidazole-2-sulfonic acid (1*H*-B-SA) (**5**) possesses both aromatic and anionic moieties known to be important for the interaction of small molecules with amyloid proteins and peptides[30].

The mass spectrum of a 10:1 molar ratio of 1*H*-B-SA and hIAPP is indicative of non-specific binding, resulting in a series of ions with multiple ligands bound, following a Poisson distribution[21,22] (Figure 4c). As an interaction of this type often involves charge, it is less sensitive to structure and can be maintained during the ESI process[22]. Additionally, these types of interactions can be more stable in the gas-phase than hydrophobic interactions[24], such as proposed for hIAPP and EGCG (**2**)[10]. Consistent with this, the ion intensity of the 1*H*-B-SA:hIAPP complex is decreased at increased ionic strength (Supplementary, Figure S2). Non-specific interactions can be distinguished from specific interactions (that show a binomial distribution[21]) by comparison of the binding profiles (Figure 1). To confirm annotation as a non-specific binding ligand, a second analysis performed at lower ligand:peptide ratio may be required to avoid ambiguity that may arise by specific binding of molecules forming multiply bound complexes at high ligand:peptide ratios.

ThT fluorescence and TEM investigation indicated that non-specific binding of 1*H*-B-SA to hIAPP does not inhibit fibril formation (Figure 4a,b). Similarly, the mass spectrum of a 10:1 molar ratio of tramiprosate (3-amino-1-propanesulfonic acid) (**6**) and hIAPP is also indicative of a non-inhibitory, non-specific interaction, which is confirmed by TEM (Supplementary, Figure S3). Importantly, for the compounds aspirin (**7**), ibuprofen (**8**), benzimidazole (**9**) and hemin (**10**) (Supplementary, Section 1 & Table S1), no evidence for binding to monomeric hIAPP, alteration in the monomer charge state distribution, or oligomer population, was observed using ESI-IMS-MS and fibrils were observed to form as shown by TEM (Supplementary, Figure S5). Previous studies using CD spectroscopy and Congo red binding assays led to the erroneous conclusion that aspirin is an inhibitor of hIAPP amyloid formation[31], illustrating how ESI-IMS-MS helps avoid false positive results.

Predicting the inhibitory potential of small molecules against amyloid formation from their structure alone is difficult, since structural analogues can show significant variability in aggregation inhibition. Rifamycin SV, for example, can block fibril formation by β_2-microglobulin (β_2m), while other rifamycins are ineffective[32]. Similarly, derviatives of EGCG have marked differences in their inhibitory capacity[33]. The LogP value (the log of the hydrophobic partition coefficient) of each small molecule tested was calculated to determine the diversity in hydrophobicity of the compounds tested and to deduce any correlation with their ability to inhibit amyloid formation (Supplementary, Figure S6). The LogP values of the positive inhibitors range from -4.4 (FG) to +2.2 (EGCG), suggesting that polarity is not the only important factor for binding. Both hydrophilic FG and hydrophobic EGCG inhibit hIAPP aggregation, confirming that the MS-based method for screening inhibitors is capable of observing both electrostatic and hydrophobic interactions between amyloidogenic peptides and aggregation inhibitors.

Further analyses using Collision Induced Dissociation (CID) MS/MS showed that the specific inhibitors bind more tightly than their non-specific counterparts, as judged by their gas-phase stability (Supplementary, Figure S7), providing an additional means of selecting ligands for further analysis. Arrival time distribution (ATD) plots from ESI-IMS-MS experiments also provide evidence for the type of interaction occurring. With FG bound, there is a shift in the ATD plot towards more compact hIAPP monomeric protein species (Supplementary, Figure S8).

Oligomer formation in the presence of small molecule inhibitors

ESI-IMS-MS was utilized to determine the individual nature and abundance of the lowly-populated hIAPP oligomers in the presence of each small molecule. In the absence of small molecule, hIAPP forms oligomers up to, and including, hexamers within 2 minutes of dilution into buffer (Figure 2c)[10]. In the presence of a 10-fold molar excess of a 'negative', non-interacting small molecule such as ibuprofen (**8**), the same array of oligomers is observed (Figure 5a). When a 'positive' specific inhibitor (e.g. FG) (**1**) is added (Figure 5b), binding of the small molecule to the peptide monomer is observed, with no higher order hIAPP species detected. This lack of oligomers is likely due to inhibition of self-assembly achieved by small molecule binding to the monomeric peptide. When a non-specific binder (e.g. 1*H*-B-SA (**5**)) is added (Figure 5c), multiple copies of ligands (≤ seven molecules) bound to each monomeric conformer are observed in the mass spectrum, indicative of a non-specific interaction. Conversely, the spectrum of hIAPP in the presence of CR (**4**) (Figure 5d) shows a multitude of higher order species. However, the majority of these peaks correspond to multimers of CR resulting from self-association of the small molecule. Peptide monomers are also observed in the spectrum but not peptide oligomers, which may result from their low intensities compared with CR aggregates, or their absence. The ESI-IMS-MS data presented reveal clear differences between the spectral 'fingerprint' of hIAPP undergoing no interaction, specific, non-specific or colloidal interactions with small molecules. Consequently, 'hits' from screens of potential small molecule inhibitors can be distinguished

readily from negative, colloidal or non-specifically bound molecules using ESI-IMS-MS and, based on simple characterization of the spectral features, selected for further characterization or optimization.

Screening mixtures of small molecules using ESI-IMS-MS

To validate the use of ESI-IMS-MS as a potential high-throughput screen (HTS) for small molecule interactions with aggregating proteins/peptides, several small molecules were mixed and added to hIAPP in combination. The ability of ESI-IMS-MS to differentiate between molecules able to bind specifically to the target protein/peptide from their non-binding or non-specific binding counterparts was then assessed. This approach has two key advantages: firstly, it decreases the time taken to screen an array of molecules (5-10 molecules/min); secondly, in competition, the strongest binders as observed in the gas-phase should out-compete negative, weak or colloidal inhibitors. This method is demonstrated using FG (positive) (**1**), CR (colloidal) (**4**), 1*H*-B-SA (non-specific) (**5**) and four small molecules that do not bind to hIAPP (negative) (**7-10**). When added to hIAPP (32 μM) in combination (160 μM each small molecule), FG and CR behave as each one behaved when added individually, i.e. FG binds specifically to the target peptide and CR self-associates without any specific protein interaction being observed (Supplementary, Figure S9). The presence of equimolar CR does not prevent FG from binding to hIAPP, nor does the presence of equimolar FG inhibit the self-association of CR. We also tested the ability of FG to bind hIAPP in the presence of mixtures of small molecules that do not bind (aspirin (**7**), ibuprofen (**8**), benzimidazole (**9**) and hemin (**10**)). The results showed that of the five small molecules present, only FG binds hIAPP (Supplementary, Figure S9). Additionally, the presence of a high concentration of a non-specifically binding small molecule did not perturb the interaction of FG with hIAPP (Supplementary, Figure S10). In the unlikely event that two positive inhibitors are encountered in the same mixture, the molecule which binds most stably in the gas-phase will out-compete the other. This is the case when FG (**1**) and EGCG (**2**) are each added in a 5-fold molar excess to hIAPP (Supplementary, Figure S10). FG and

hIAPP have favourable electrostatic interactions[25], whereas EGCG is thought to bind principally via hydrophobic interactions[34]. Given the known ability of electrostatic interactions to be preserved in the gas-phase over their hydrophobic counterparts, FG out-competes EGCG. The relative affinity of these two different ligands for hIAPP therefore cannot be deduced from these data. To control for the effects of the chemistry of binding determining the relative intensity of bound peaks observed by ESI-MS[22,23], the K_d of small molecules identified as a "hit" in a mixture of compounds should be confirmed using other biophysical methods in solution.

ESI-IMS-MS as a generic screen for amyloid inhibitors

To demonstrate the applicability of ESI-IMS-MS as a generic tool for screening and classifying inhibitors of aggregating systems, we screened for inhibitors of Aβ40 assembly[1]. The sequences of hIAPP (Figure 2a) and Aβ40 (Figure 6a) share 25 % identity and 50 % similarity, with the core sequences Aβ40 (26–32) and hIAPP (21–27) believed to be involved in the self-assembly of each peptide[35-37] being most similar. Aβ40 (32 μM) was incubated alone or with tramiprosate (**6**), hemin (**10**) or EGCG (**2**) at 10:1 molar ratio of small molecule to Aβ40. Aβ40 alone, when analyzed by ESI-MS, gives rise to dominant 3+ and 4+ monomer charge state ions (Figure 6b) and oligomeric species from dimer through pentamer (Figure 6c) *en route* to long straight amyloid fibrils.

Tramiprosate (**6**) has been shown to retard Aβ40 and Aβ42 fibrillation *in vivo*, likely *via* competition with glycosaminoglycan (GAG) binding to the peptide[38,39]. The mass spectrum of a 10:1 molar ratio of tramiprosate:Aβ40 peptide (Figure 6d) indicates a non-specific interaction which may explain how tramiprosate interferes with GAG binding to Aβ *in vivo*[38]. ThT and TEM data reveal fibrillation in the absence and presence of tramiprosate (**6**) (Figures 6e,f), corroborating these findings. Hemin (**10**) (along with other porphyrins) has also been reported to interfere with Aβ fibrillation[17,40]. Here, hemin has no observed effect on Aβ self-assembly as judged by its inability to bind to Aβ40 (Figure 6d) and the resultant

formation of fibrils (Figure 6f). Notably, no increase in ThT fluorescence is observed in the presence of hemin, presumably because the small molecule either interferes with ThT fluorescence or prevents ThT binding (Figure 6e). Conversely, EGCG (**2**), binds specifically to Aβ40 monomer, forming a 1:1 EGCG:Aβ40 complex (Figure 6d), resulting in the formation of amorphous aggregates and the absence of long straight amyloid fibrils (Figures 6e,f). The results demonstrate, therefore, the utility of ESI-MS as a screen for inhibitors of different amyloid systems.

Focused screen for the identification of novel inhibitors of amyloid formation

To validate further the MS-based assays, we next performed a screen of a library of novel molecules with structural similarity to the aggregation inhibitors previously reported (Supplementary, Table S2). We reasoned that a focussed screen of this type would be a rigorous test for the ESI-IMS-MS assay and indicate the suitability of this approach for HTS. Focused screening is a well-versed method to improve the hit-rate of a HTS by seeding a screening library with compounds which have a higher probability to inhibit, or bind to, the target compared with random screening[41]. The screening method uses the structural information from known bioactive ligands to identify novel compounds with similar structure, and hence potential biological activity. For proof of principle, five known inhibitors of hIAPP and/or Aβ40 aggregation (vanillin[42], resveratrol[43], curcumin[44], chloronaphthoquinine-tryptophan[45] and EGCG[10]) were selected as queries to seed a focussed library of compounds for screening. The seeding process involved assessment of each of the inhibitors for structural similarity to an in-house, structurally diverse library of 50,000 lead-like small molecules using the programme Rapid Overlay of Chemical Structures (ROCS)[46]. A subset of 20 compounds was then chosen for analysis using the comparator (ROCS Combiscore) with consideration to maximal structural diversity of the proposed screening set. The 20 compounds (molecules 11-30) selected were screened, together with compounds 31-40 which have been reported to inhibit other forms of fibrillogenesis by other

polypeptides (Supplementary, Table S2). LogP values of these compounds are shown in Supplementary, Figure S11.

Of these 30 compounds screened, one was found to inhibit hIAPP aggregation (compound **26**), three demonstrated non-specific binding to hIAPP (compounds **13**, **25** and **27**) and the remainder did not bind (Supplementary, Table S2). The newly disovered inhibitor (compound **26**) is a non-obvious structural mimetic of chloronaphthoquinine–tryptophan (Supplementary, Figure S12). In the presence of a 10-fold molar excess of compound **26**, hIAPP monomer shows evidence of specific ligand binding, fibril formation is inhibited and amorphous aggregates result (Supplementary, Figure S13).

<Uncaptioned graphic structures 26 13 25 and 27> to be placed here

Automation of ESI-MS allows identification of novel compounds from focussed libraries in the form of a semi-HTS. For proof of principle, we performed analyses from a 96-well plate format, with data acquisitions of one minute per well. The results demonstrate that spectra of high quality can be obtained in a reproducible manner (Supplementary, Figure S14). With this method, 96 novel potential inhibitors could be screened per plate, consuming ~1 mg peptide. Using robotic automation, ~1000 compounds can be screened in less than 24 hours. By assaying mixtures of five compounds in parallel, 480 molecules could be screened per plate, increasing the screening rate to ~5000 novel compounds per day.

Conclusions

The data presented demonstrate the use of ESI-IMS-MS as a HTS for inhibitors of amyloid assembly. This approach allows rapid identification of protein-ligand interactions, using microliter sample volumes and milligrams of protein, and provides information-rich data concerning the identity of the interacting species (monomer or oligomer), the nature of binding (specific, non-specific or colloidal) and the effect of the ligand on protein aggregation (monomer binding, shift in monomer conformational equilibrium, disassembly of oligomers). The use of IMS in conjunction with ESI-MS serves further to allow a reliable and easily interpretable screen based purely on the appearance of 3D Driftscope plots, without requiring complex data analysis. The results establish this method as a powerful tool with unique analytical capability for the discovery of small molecule leads in the drug discovery field. Additionally, a novel inhibitor of hIAPP aggregation has been identified based on analysis of a library of small molecules, illustrating the potential of this method as a HTS.

Methods

Sample preparation for MS

hIAPP was synthesized using Fmoc chemistry, oxidised using dimethyl sulfoxide (DMSO) to form the disulfide bond linking residues Cys 2 – Cys 7, and purified via HPLC. Hydrochloric acid was used as the counter ion in all HPLC buffers as trifluoroacetic acid can affect the kinetics of amyloid formation[47] (see Supplementary, Section 2 for further details). Aβ40 was expressed recombinantly in *E. coli* (Supplementary, Section 2). Lyophilized hIAPP samples were dissolved in DMSO at a final peptide concentration of 3.2 mM. After 24 h incubation at 25 ℃, stock solutions were diluted 100 -fold into 200 mM ammonium acetate, pH 6.8, to a final peptide concentration of 32 μM for MS analysis. The final concentration of DMSO was 1 % (*v/v*). Lyophilized Aβ40 was dissolved at 32 μM in 200 mM ammonium acetate, pH 6.8, 1 % DMSO (*v/v*), and centrifuged at 13,000 *g*, 4 ℃ for 10 min prior to analysis. All samples were incubated at 25 ℃ in 96 -well plates without agitation.

ESI-(IMS)-MS analysis

A Synapt HDMS quadrupole-time-of-flight mass spectrometer (Micromass UK Ltd., Waters Corpn., Manchester, UK), equipped with a Triversa NanoMate (Advion Biosciences, Ithaca, NY, USA) automated nano-ESI (nESI) interface, was used for these analyses. The instrument has a traveling-wave IMS device situated in between the quadrupole and the time-of-flight analyzers, and has been described in detail elsewhere[48]. hIAPP or Aβ40 samples were analyzed using positive ionization nESI with a capillary voltage of 1.7 kV and a nitrogen nebulizing gas pressure of 0.8 psi. The following instrumental parameters were used: cone voltage 30 V; source temperature 60 ℃; backing pressure 1.6 mBar; ramped traveling wave height 7–20 V; traveling wave speed 300 m/s; IMS nitrogen gas flow 20 mL/min; IMS cell pressure 0.55 mBar. Data were processed by use of MassLynx v4.1 and Driftscope software supplied with the mass spectrometer. The *m/z* scale was calibrated with aq. CsI cluster ions.

Collision induced dissociation (CID) tandem mass spectrometry (MS/MS) was carried out in the trap collision cell of the mass spectrometer, using argon gas. The quadrupole analyzer was used to select ions representing ligand-bound monomer complexes and increasing collision energy was applied to the trap collision cell in 10 V increments from 10-100 V, until the ligands were completely dissociated from the monomer ions. Automation of the NanoMate for high throughput experiments was programmed enabling samples in each of the 96-wells to be analyzed for one minute, consecutively.

For analysis of ligand binding to monomeric peptide, hIAPP or Aβ40 (32 μM) was dissolved in 200 mM ammonium acetate (pH 6.8) containing 32 μM or 320 μM of small molecule. For analysis of these samples by nESI-MS, a cone voltage of 30 V was used to preserve protein-ligand interactions, and a backing pressure of 1.6 mbar was applied. Data were acquired over the range *m/z* 200–6,000.

Thioflavin-T (ThT) fluorescence assays

Samples were added to a 96-well plate (Corning Costar 3915, Corning Life Sciences, Amsterdam, The Netherlands), sealed with clear sealing film and incubated in a FLUOstar OPTIMA plate reader (BMG Labtech, Aylesbury, Bucks, UK) for 5 days at 25 ℃ without agitation. Each 100 μL sample contained ThT (100 μM) and peptide (32 μM) in 200 mM ammonium acetate, pH 6.8 and a 1 % (*v/v*) final concentration of DMSO. The thioflavin-T studies used excitation and emission filters of 430 and 485 nm, respectively.

Transmission electron microscopy (TEM)

The TEM images of each 32 μM peptide solution were acquired after 5 days incubation at 25 ℃ using a JEM-1400 (JEOL Ltd., Tokyo, Japan) transmission electron microscope. Carbon grids were prepared by irradiation under UV light for 30 min and stained with 4 % (*w/v*) uranyl acetate solution as described previously[49].

Virtual screening

The structure of each of the five query molecules (vanillin, resveratrol, curcumin, chloronaphthoquinine-tryptophan and epigallocatechin-3-gallate (EGCG)) was minimized to the lowest energy conformer using LigPrep[50]. The minimized conformers were used as the query scaffold for virtual screening of an in-house library of 50,000 structurally diverse, novel small molecules using Rapid Overlay of Chemical Structures (ROCS)[46]. ROCS is a 3D method that matches the shape of a molecule to the shape of the query molecule. It also incorporates pharmacophoric features in assessing overlays such that the *ROCS Combiscore* measures the similarity of the matched shapes as well as the matched pharmacophoric features. Virtual hits were pooled and ranked according to the *ROCS Combiscore* parameter and 20 of the top 100 compounds were selected for screening based on a qualitative assessment of structural diversity. In addition, a further ten compunds chosen from the literature as known inhibitors of amyloid formation by different polypeptide sequences were included in the screen.

Acknowledgements

L.M.Y. is funded by a Biotechnology and Biological Sciences Research Council (BBSRC) CASE studentship (Grant Number BB/I015361/1) sponsored by Micromass UK Ltd/Waters Corpn, Manchester, UK. J.C.S. is funded by a BBSRC CASE studentship (Grant Number BB/H014713/1) sponsored by Avacta Analytical PLC, Wetherby, UK. R.A.M. is funded by a BBSRC studentship (Grant Number BB/F01614X/1). The Synapt HDMS mass spectrometer was purchased with funds from the Biotechnology and Biological Sciences Research Council through its Research Equipment Initiative scheme (BB/E012558/1). S.E.R. acknowledges funding from the European Research Council under the European Union's Seventh Framework Programme (FP7/2007-2013; 322408). D.P.R. acknowledges support from the United States National Institutes of Health (GM078114). We thank Dominic Walsh (Brigham & Women's Hospital, Boston, USA) and Sara Linse (Lund University, Sweden) for provision of Aβ40 peptide and vector and Dr James R. Ault (University of Leeds) for setting up the

automated ESI-MS analyses. We also acknowledge all members of the Ashcroft, Radford and Raleigh groups for helpful discussions.

Correspondence and requests for materials should be addressed to A.E.A. and S.E.R.

Author contributions

L.M.Y. and J.C.S. contributed equally to this work. L.M.Y., J.C.S., S.E.R. and A.E.A. conceived and designed the experiments. L.M.Y., J.C.S. and R.A.M. performed the experiments; C.H.R. and R.J.F designed and prepared the screening library. L.H.T. and D.P.R. prepared hIAPP. L.M.Y. analyzed the data. L.M.Y., J.C.S., R.A.M., C.H.R., R.J.F., L.H.T., D.P.R. S.E.R. and A.E.A. wrote the manuscript. All authors discussed the results and commented on the manuscript.

Competing financial interests

The authors declare no competing financial interests.

Figure Legends

Figure 1. Schematic diagram of the basis of the ESI-IMS-MS screen and a selection of the small molecules utilized for screen validation. (a-d) Schematic of expected ESI mass spectra resulting from different interactions between peptide/protein monomer (denoted m) and potential inhibitors (denoted L). Oligomers are denoted o; charge states are in superscript. (a) A specific ligand (termed positive) will result in a binomial distribution of bound peaks (pink)[21]; (b) the presence of a colloidal inhibitor will lead to spectra containing overlapping peaks resulting from the heterogeneous self-association of the small molecule (orange peaks); (c) a non-specific ligand will bind and result in a Poisson distribution of bound peaks (green)[21]; (d) the presence of a non-interacting small molecule (termed negative) will result in spectra similar to those of peptide alone; (e) list of ten small molecules analyzed initially for inhibition of hIAPP aggregation during ESI-MS screen validation. Colors correspond to binding-mode classification by mass spectra (a-d): specific = pink, colloidal = orange, non-specific = green, negative = gray.

Figure 2. hIAPP forms an array of oligomeric species en route to long-straight amyloid fibrils. (a) Primary sequence of hIAPP. The peptide has a disulfide bridge between Cys-2 and Cys-7 and an amidated C-terminus; (b) ESI-MS mass spectrum of hIAPP. Numbers above peaks denote oligomer order, with the positive charge state of ions in superscript; (c) ESI-IMS-MS Driftscope plot of the hIAPP monomer (1) through hexamer (6), present 2 min after diluting the monomer to a final peptide concentration of 32 μM in 200 mM ammonium acetate, pH 6.8. ESI-IMS-MS Driftscope plots show IMS drift time versus mass/charge (m/z) versus intensity (z = square root scale). Inset: negative stain TEM image of hIAPP fibrils after 5 days in 200 mM ammonium acetate pH 6.8 buffer (25 ℃, quiescent) (scale bar = 100 nm).

Figure 3. Inhibition of hIAPP amyloid assembly by Fast Green FCF (FG). (a) ThT fluorescence intensity over time of hIAPP alone (black circles) (32 μM peptide, 200 mM

ammonium acetate buffer, pH 6.8, 25 ℃, quiescent) and with increasing FG:hIAPP molar ratios: 1:1 (orange) and 10:1 (green), showing dose dependent decrease in formation of ThT-positive hIAPP species upon addition of FG. (b) Negative stain TEM images of hIAPP incubated with (i) 1:1 or (ii) 10:1 molar ratios of FG:hIAPP for 5 days (25 ℃, quiescent) (scale bar = 100 nm), showing lack of fibrillation (ii) and formation of small/amorphous aggregates (i) of hIAPP in the presence of FG. (c) Positive ion ESI mass spectra showing FG alone (i), or added at 32 μM (ii), or 320 μM (iii), to hIAPP (32 μM). FG binds to the 2+ and 3+ charge state ions of hIAPP monomer (bound peaks denoted with orange or green circles; number of circles represents number of ligands bound), and to the 4+ charge state of the hIAPP dimer (bound peak denoted with white circle). This binding mode is classified as specific.

Figure 4. Colloidal inhibition and non-specific binding observed using ESI-IMS-MS. (a) ThT fluorescence intensity of hIAPP (black) (32 μM peptide, 200 mM ammonium acetate buffer, pH 6.8, 25 ℃, quiescent) with Congo red (CR):hIAPP molar ratios: 1:1 (orange) and 10:1 (red) and with 1H-benzimidazole-2-sulfonic acid (1*H*-B-SA):hIAPP molar ratio: 10:1 (blue)). Inhibition of the formation of ThT-positive species is observed only in the presence of excess CR. (b) Negative stain TEM images of hIAPP incubated with 1:1 (i) or 10:1 (ii) molar ratios of CR or a 10:1 molar ratio of 1H-B-SA (iii) (5 days, 25 ℃, quiescent) (scale bar = 100 nm). Fibrils are observed in the presence of equimolar CR and excess 1*H*-B-SA but not in the presence of excess CR. (c) Positive ion ESI mass spectra showing CR added at 32 μM (i) or 320 μM (ii), or 1*H*-B-SA added at 320 μM (iii), to hIAPP (32 μM). CR is not observed to bind to hIAPP when added at 32 μM (i) or 320 μM (ii), however CR self-aggregates at 320 μM (ii) (denoted n^{x+}, where n is the number of CR molecules and x is the charge state of those ions (red peaks). This binding mode is classified as colloidal. Multiple copies of 1*H*-B-SA bind to the 2+ and 3+ hIAPP monomer ions (bound peaks denoted with blue circles, number of circles represents number of ligands bound), and to the hIAPP dimer (bound peaks denoted with white circles). This binding mode is classified as non-specific.

Figure 5. ESI-IMS-MS demonstrates the mode of inhibition (specific/colloidal/non-specific) or lack of inhibition of hIAPP amyloid formation by small molecules. ESI-IMS-MS Driftscope plots of hIAPP and (a) ibuprofen; (b) FG (bound peaks denoted with yellow (1^{3+} bound) or green (1^{2+} bound) circles, number of circles represents number of ligands bound); (c) 1H-B-SA (bound peaks denoted with blue circles; and (d) CR (colloidal aggregates are denoted n^{x+}, where n is the number of CR molecules and x is the charge state of the aggregate) (320 μM small molecule) to hIAPP (32 μM). An example of a negative (a), a positive (b), a non-specific (c) and a colloidal inhibitor (d) are illustrated. The numbers on the Driftscope plots indicate the oligomer order and the adjacent superscripted numbers show the charge state of those ions.

Figure 6. Aβ40 alone and with non-specific, negative and specific binding small molecules. (a) Primary sequence of recombinantly expressed Aβ40 (with an additional N-terminal methionine); (b) ESI mass spectrum of Aβ40. Numbers adjacent to peaks denote oligomer order, with the positive charge state of the ions in superscript; (c) ESI-IMS-MS Driftscope plot of Aβ40 alone (32 μM in 200 mM ammonium acetate, pH 6.8) showing IMS drift time versus *m/z* versus intensity (z = square root scale); (d) positive ion ESI mass spectra showing 320 μM tramiprosate (i), hemin (ii) or EGCG (iii) added to Aβ40 peptide (32 μM). Tramiprosate binds multiple copies to the 3+ and 4+ ions of Aβ40 monomer (bound peaks denoted with pink circles, number of circles represents number of ligands bound).This binding mode is classified as non-specific. Hemin (ii) does not bind and is classified as negative; EGCG (iii) binds to both the 3+ and 4+ ions of Aβ40 monomer (bound peaks are denoted with blue circles) and is classified as specific. (e) ThT fluorescence intensity of Aβ40 alone (black circles) in the presence of tramiprosate (pink circles), EGCG (blue circles) or hemin (orange circles) at small molecule:Aβ40 molar ratios of 10:1. Inhibition of the formation of ThT-positive species is observed in the presence of excess EGCG and interference with ThT fluorescence is observed in the presence of excess hemin. (f)

Negative stain TEM images of Aβ40 alone (i) or incubated with 10:1 molar ratios of tramiprosate (ii), hemin (iii) or EGCG (iv) (5 days, 25 ℃, quiescent); scale bar = 100 nm. Fibrils are observed by Aβ40 alone and in the presence of excess tramiprosate and hemin but not in the presence of excess EGCG.

References

1. Sipe, J. D. et al. Amyloid fibril protein nomenclature: 2012 recommendations from the Nomenclature Committee of the International Society of Amyloidosis. *Amyloid* **19**, 167-170 (2012).
2. Grimster, N. P. et al. Aromatic sulfonyl fluorides covalently kinetically stabilize transthyretin to prevent amyloidogenesis while affording a fluorescent conjugate. *J. Amer. Chem. Soc.* **135**, 5656-5668 (2013).
3. Klabunde, T. et al. Rational design of potent human transthyretin amyloid disease inhibitors. *Nat. Struct. Mol. Biol.* **7**, 312-321 (2000).
4. Connelly, S., Choi, S., Johnson, S. M., Kelly, J. W. & Wilson, I. A. Structure-based design of kinetic stabilizers that ameliorate the transthyretin amyloidoses. *Curr. Opin. Struct. Biol.* **20**, 54-62 (2010).
5. Hamrang, Z., Rattray, N. J. W. & Pluen, A. Proteins behaving badly: emerging technologies in profiling biopharmaceutical aggregation. *Trends Biotech.* **31**, 448-458 (2013).
6. Meier, J. J. et al. Inhibition of human IAPP fibril formation does not prevent β-cell death: Evidence for distinct actions of oligomers and fibrils of human IAPP. *Am. J. Physiol. Endocrinol. Metab.* **291**, E1317-E1324 (2006).
7. Aitken, J. F., Loomes, K. M., Konarkowska, B. & Cooper, G. J. S. Suppression by polycyclic compounds of the conversion of human amylin into insoluble amyloid. *Biochem. J.* **374**, 779-784 (2003).
8. Harroun, T. A., Bradshaw, J. P. & Ashley, R. H. Inhibitors can arrest the membrane activity of human islet amyloid polypeptide independently of amyloid formation. *FEBS Letts.* **507**, 200-204 (2001).
9. Woods, L. A. et al. Ligand binding to distinct states diverts aggregation of an amyloid-forming protein. *Nat. Chem. Biol.* **7**, 730-739 (2011).
10. Young, L. M., Cao, P., Raleigh, D. P., Ashcroft, A. E. & Radford, S. E. Ion mobility spectrometry-mass spectrometry defines the oligomeric intermediates in amylin amyloid formation and the mode of action of inhibitors. *J. Amer. Chem. Soc.* **136**, 660-670 (2014).
11. Hyung, S. J. et al. Insights into antiamyloidogenic properties of the green tea extract (-)-epigallocatechin-3-gallate toward metal-associated amyloid-β species. *Proc. Natl. Acad. Sci. U.S.A.* **110**, 3743-3748 (2013).
12. Westermark, P. Amyloid in the islets of Langerhans: thoughts and some historical aspects. *Ups. J. Med. Sci.* **116**, 81-89 (2011).

13. Selkoe, D. J. Alzheimer's disease: Genes, proteins, and therapy. *Physiol. Rev.* **81**, 741-766 (2001).
14. Feng, B. Y. et al. Small-molecule aggregates inhibit amyloid polymerization. *Nat. Chem. Biol.* **4**, 197-199 (2008).
15. Bieschke, J. et al. EGCG remodels mature α-synuclein and amyloid-β fibrils and reduces cellular toxicity. *Proc. Natl. Acad. Sci. U.S.A.* **107**, 7710-7715 (2010).
16. Meng, F., Abedini, A., Plesner, A., Verchere, C. B. & Raleigh, D. P. The flavanol (-)-epigallocatechin 3-gallate inhibits amyloid formation by islet amyloid polypeptide, disaggregates amyloid fibrils, and protects cultured cells against IAPP-induced toxicity. *Biochem.* **49**, 8127-8133 (2010).
17. Howlett, D., Cutler, P., Heales, S. & Camilleri, P. Hemin and related porphyrins inhibit β-amyloid aggregation. *FEBS Letts.* **417**, 249-251 (1997).
18. Meng, F. & Raleigh, D. P. Inhibition of glycosaminoglycan-mediated amyloid formation by islet amyloid polypeptide and proIAPP processing intermediates. *J. Mol. Biol.* **406**, 491-502 (2010).
19. Porat, Y., Mazor, Y., Efrat, S. & Gazit, E. Inhibition of islet amyloid polypeptide fibril formation: a potential role for heteroaromatic interactions. *Biochem.* **43**, 14454-14462 (2004).
20. Ehrnhoefer, D. E. et al. EGCG redirects amyloidogenic polypeptides into unstructured, off-pathway oligomers. *Nat. Struct. Mol. Biol.* **15**, 558-566 (2008).
21. Daubenfeld, T., Bouin, A. P. & van der Rest, G. A deconvolution method for the separation of specific versus nonspecific interactions in noncovalent protein-ligand complexes analyzed by ESI-FT-ICR mass spectrometry. *J. Am. Soc. Mass Spectrom.* **17**, 1239-1248 (2006).
22. Sun, N., Sun, J., Kitova, E. N. & Klassen, J. S. Identifying nonspecific ligand binding in electrospray ionization mass spectrometry using the reporter molecule method. *J. Am. Soc. Mass Spectrom.* **20**, 1242-1250 (2009).
23. Sun, J., Kitova, E. N., Wang, W. & Klassen, J. S. Method for distinguishing specific from nonspecific protein-ligand complexes in nanoelectrospray ionization mass spectrometry. *Anal. Chem.* **78**, 3010-3018 (2006).
24. Wang, W., Kitova, E. N. & Klassen, J. S. Influence of solution and gas phase processes on protein-carbohydrate binding affinities determined by nanoelectrospray Fourier transform ion cyclotron resonance mass spectrometry. *Anal. Chem.* **75**, 4945-4955 (2003).
25. Meng, F. et al. The sulfated triphenyl methane derivative acid fuchsin is a potent inhibitor of amyloid formation by human islet amyloid polypeptide and protects against the toxic effects of amyloid formation. *J. Mol. Biol.* **400**, 555-566 (2010).

26. Dupuis, N. F., Wu, C., Shea, J. E. & Bowers, M. T. Human islet amyloid polypeptide monomers form ordered beta-hairpins: a possible direct amyloidogenic precursor. *J. Amer. Chem. Soc.* **131**, 18283-18292 (2009).
27. Cheng, B. et al. Silibinin inhibits the toxic aggregation of human islet amyloid polypeptide. *Biochem. Biophys. Res. Commun.* **419**, 495-499 (2012).
28. Khurana, R., Uversky, V. N., Nielsen, L. & Fink, A. L. Is Congo red an amyloid-specific dye? *J. Biol. Chem.* **276**, 22715-22721 (2001).
29. Kim, Y. S., Randolph, T. W., Manning, M. C., Stevens, F. J. & Carpenter, J. F. Congo red populates partially unfolded states of an amyloidogenic protein to enhance aggregation and amyloid fibril formation. *J. Biol. Chem.* **278**, 10842-10850 (2003).
30. Porat, Y., Abramowitz, A. & Gazit, E. Inhibition of amyloid fibril formation by polyphenols: structural similarity and aromatic interactions as a common inhibition mechanism. *Chem. Biol. Drug. Des.* **67**, 27-37 (2006).
31. Thomas, T., Nadackal, G. T. & Thomas, K. Aspirin and diabetes: inhibition of amylin aggregation by nonsteroidal anti-inflammatory drugs. *Exp. Clin. Endocrinol. Diabetes* **111**, 8-11 (2003).
32. Woods, L. A. et al. Ligand binding to distinct states diverts aggregation of an amyloid-forming protein. *Nat. Chem. Biol.* **7**, 730-739 (2011).
33. Cao, P. & Raleigh, D. P. Analysis of the inhibition and remodeling of islet amyloid polypeptide amyloid fibers by flavanols. *Biochem.* **51**, 2670-2683 (2012).
34. Palhano, F. L., Lee, J., Grimster, N. P. & Kelly, J. W. Toward the molecular mechanism(s) by which EGCG treatment remodels mature amyloid fibrils. *J. Amer. Chem. Soc.* **135**, 7503-7510 (2013).
35. Tenidis, K. et al. Identification of a penta- and hexapeptide of islet amyloid polypeptide (IAPP) with amyloidogenic and cytotoxic properties. *J. Mol. Biol.* **295**, 1055-1071 (2000).
36. Petkova, A. T. et al. A structural model for Alzheimer's β-amyloid fibrils based on experimental constraints from solid state NMR. *Proc. Natl. Acad. Sci. U.S.A.* **99**, 16742-16747 (2002).
37. Young, L. et al. Monitoring oligomer formation from self-aggregating amylin peptides using ESI-IMS-MS. *Int. J. Ion Mobil. Spectrom.* **16**, 29-39 (2013).
38. Aisen, P. et al. Alzhemed: A potential treatment for Alzheimer's disease. *Curr. Alzheimer Res.* **4**, 473-478 (2007).
39. Gervais, F. et al. Targeting soluble Aβ peptide with Tramiprosate for the treatment of brain amyloidosis. *Neurobiol. Aging* **28**, 537-547 (2007).

40. Necula, M., Kayed, R., Milton, S. & Glabe, C. G. Small molecule inhibitors of aggregation indicate that amyloid β oligomerization and fibrillization pathways are independent and distinct. *J. Biol. Chem.* **282**, 10311-10324 (2007).
41. Valler, M. J. & Green, D. Diversity screening versus focussed screening in drug discovery. *Drug Discov. Today* **5**, 286-293 (2000).
42. De Felice, F. G. et al. Targeting the neurotoxic species in Alzheimer's disease: inhibitors of Aβ oligomerization. *The FASEB Journal* **18**, 1366-1372 (2004).
43. Ladiwala, A. R. A. et al. Resveratrol selectively remodels soluble oligomers and fibrils of amyloid Aβ into off-pathway conformers. *J. Biol. Chem.* **285**, 24228-24237 (2010).
44. Yang, F. et al. Curcumin inhibits formation of amyloid β oligomers and fibrils, binds plaques, and reduces amyloid *in vivo*. *J. Biol. Chem.* **280**, 5892-5901 (2005).
45. Scherzer-Attali, R. et al. Complete phenotypic recovery of an Alzheimer's disease model by a quinone-tryptophan hybrid aggregation inhibitor. *PLoS ONE* **5**, e11101 (2010).
46. Rapid Overlay of Chemical Structures (ROCS). http://www.eyesopen.com/ (OpenEye, Scientific Software, Santa Fe, NM, USA).
47. Marek, P., Woys, A. M., Sutton, K., Zanni, M. T. & Raleigh, D. P. Efficient microwave-assisted synthesis of human islet amyloid polypeptide designed to facilitate the specific incorporation of labeled amino acids. *Org. Letts.* **12**, 4848-4851 (2010).
48. Giles, K. et al. Applications of a travelling wave-based radio-frequency-only stacked ring ion guide. *Rapid Commun. Mass Spectrom.* **18**, 2401-2414 (2004).
49. Platt, G. W., Routledge, K. E., Homans, S. W. & Radford, S. E. Fibril growth kinetics reveal a region of beta2-microglobulin important for nucleation and elongation of aggregation. *J. Mol. Biol.* **378**, 251-263 (2008).
50. Maestro. in *Schrödinger Release* 9.3 edn (Schrödinger, LLC, NY, USA, 2014-2).

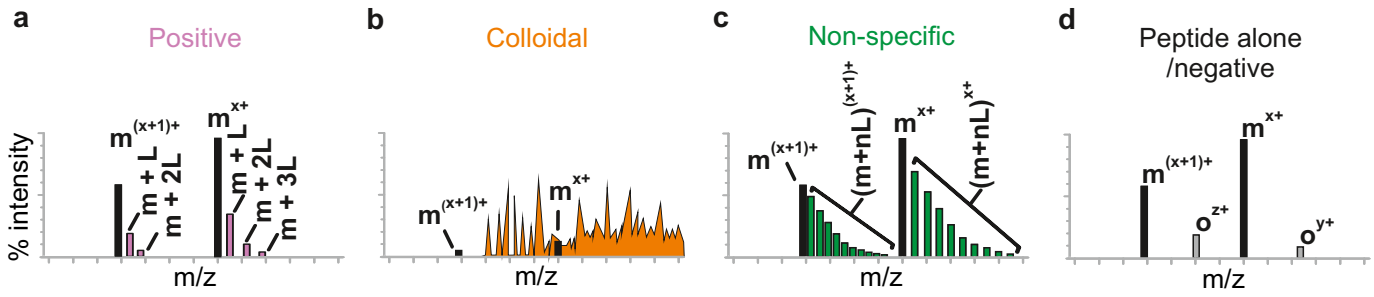

e

Mol N°	Small molecule	Structure
1	Fast green FCF	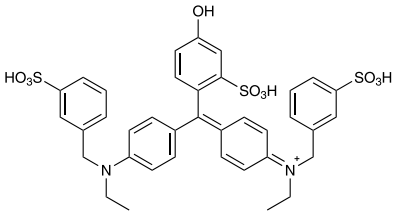
2	EGCG	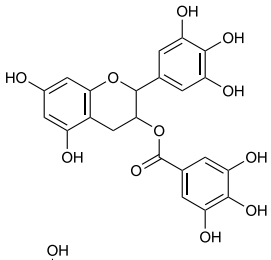
3	Silibinin	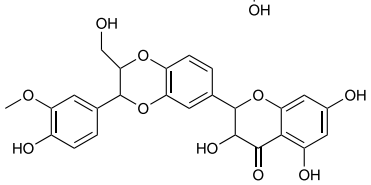
4	Congo red	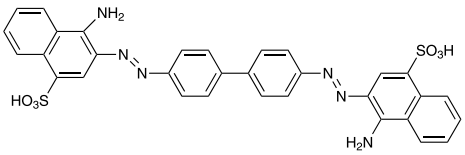

Mol N°	Small molecule	Structure
5	1*H*-benzimidazole-2-sulfonic acid	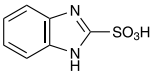
6	Tramiprosate	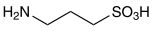
7	Aspirin	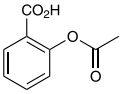
8	Ibuprofen	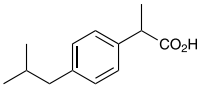
9	Benzimidazole	
10	Hemin	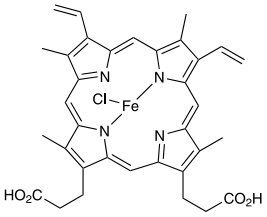

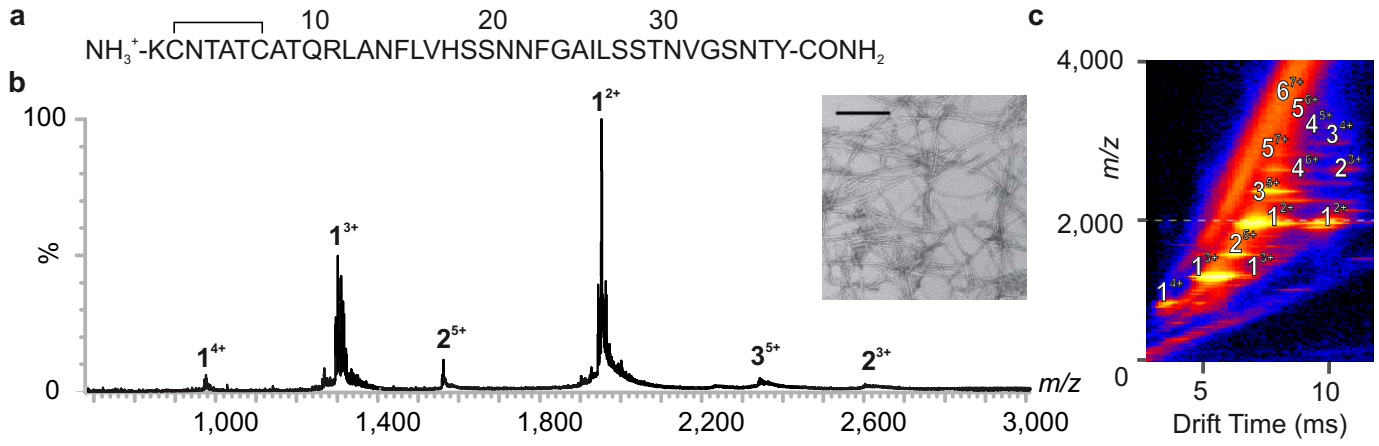
a
10
20
30
NH3+-KCNTATCATQRLANFLVHSSNNFGAILSSTNVGSNTY-CONH2
b
100
%
0
1,000
1,400
1,800
2,200
2,600
3,000
m/z
1 4+
1 3+
2 5+
1 2+
3 5+
2 3+
c
4,000
2,000
0
m/z
5
10
Drift Time (ms)

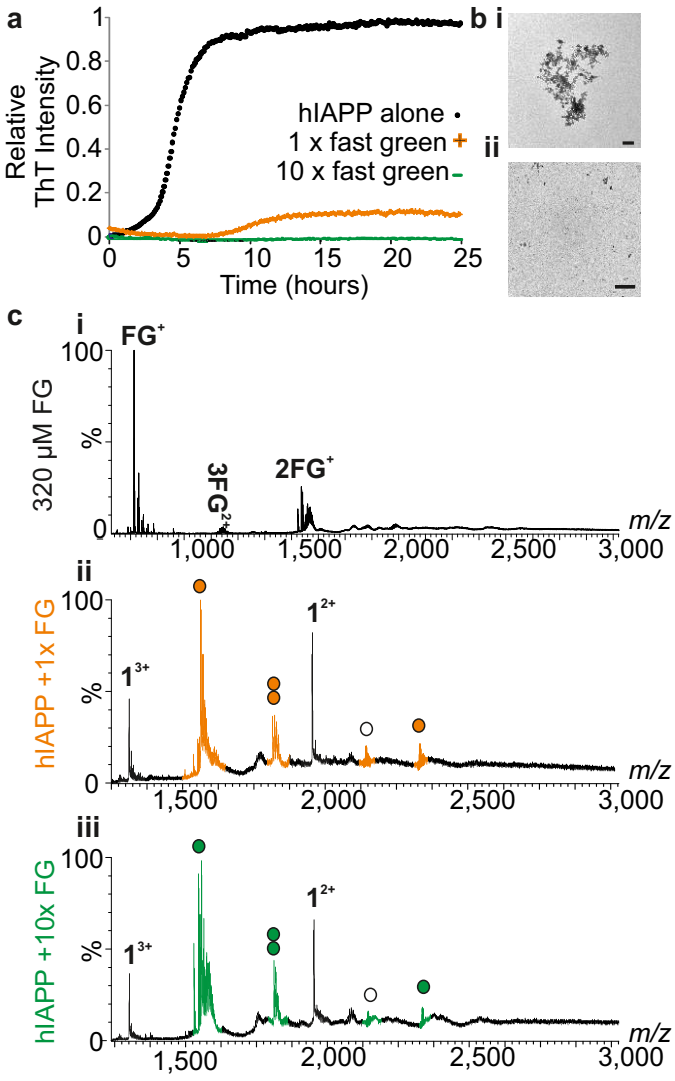
a
b i
ii
Relative ThT Intensity
hIAPP alone
1 x fast green
10 x fast green
Time (hours)
c
i
ii
iii
320 µM FG
hIAPP +1x FG
hIAPP +10x FG
FG+
3FG2+
2FG+
1 3+
1 2+
m/z
%

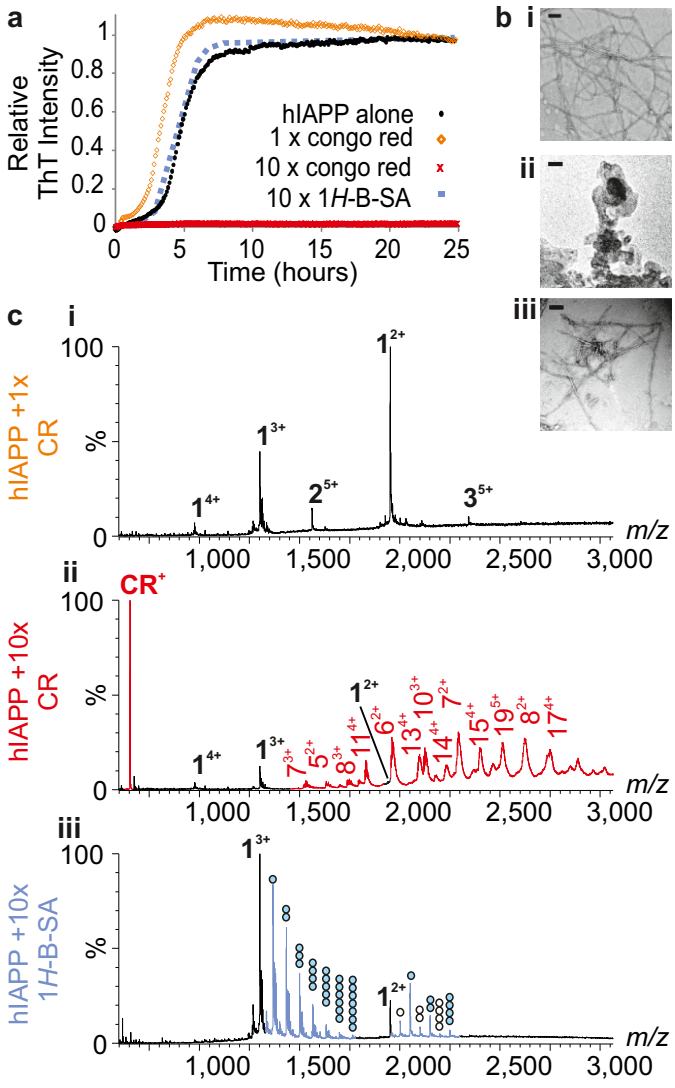
a
Relative ThT Intensity
Time (hours)
hIAPP alone
1 x congo red
10 x congo red
10 x 1H-B-SA
b i
ii
iii
c i
hIAPP +1x CR
ii
hIAPP +10x CR
CR+
iii
hIAPP +10x 1H-B-SA
m/z
%

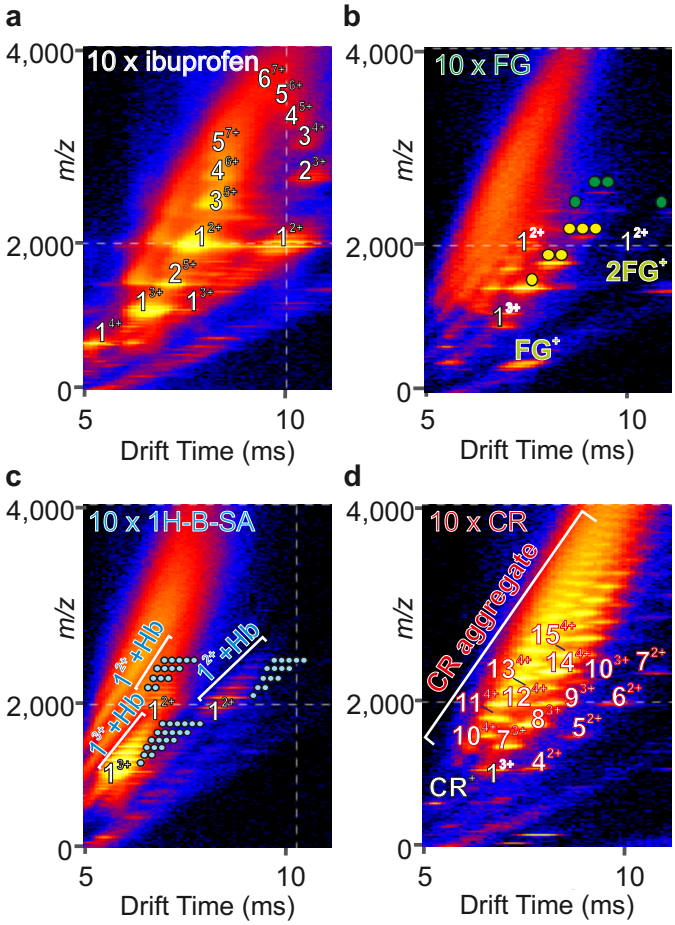
a
10 x ibuprofen
b
10 x FG
2FG+
FG+
c
10 x 1H-B-SA
1+Hb
d
10 x CR
CR aggregate
CR+
m/z
Drift Time (ms)
4,000
2,000
0
5
10

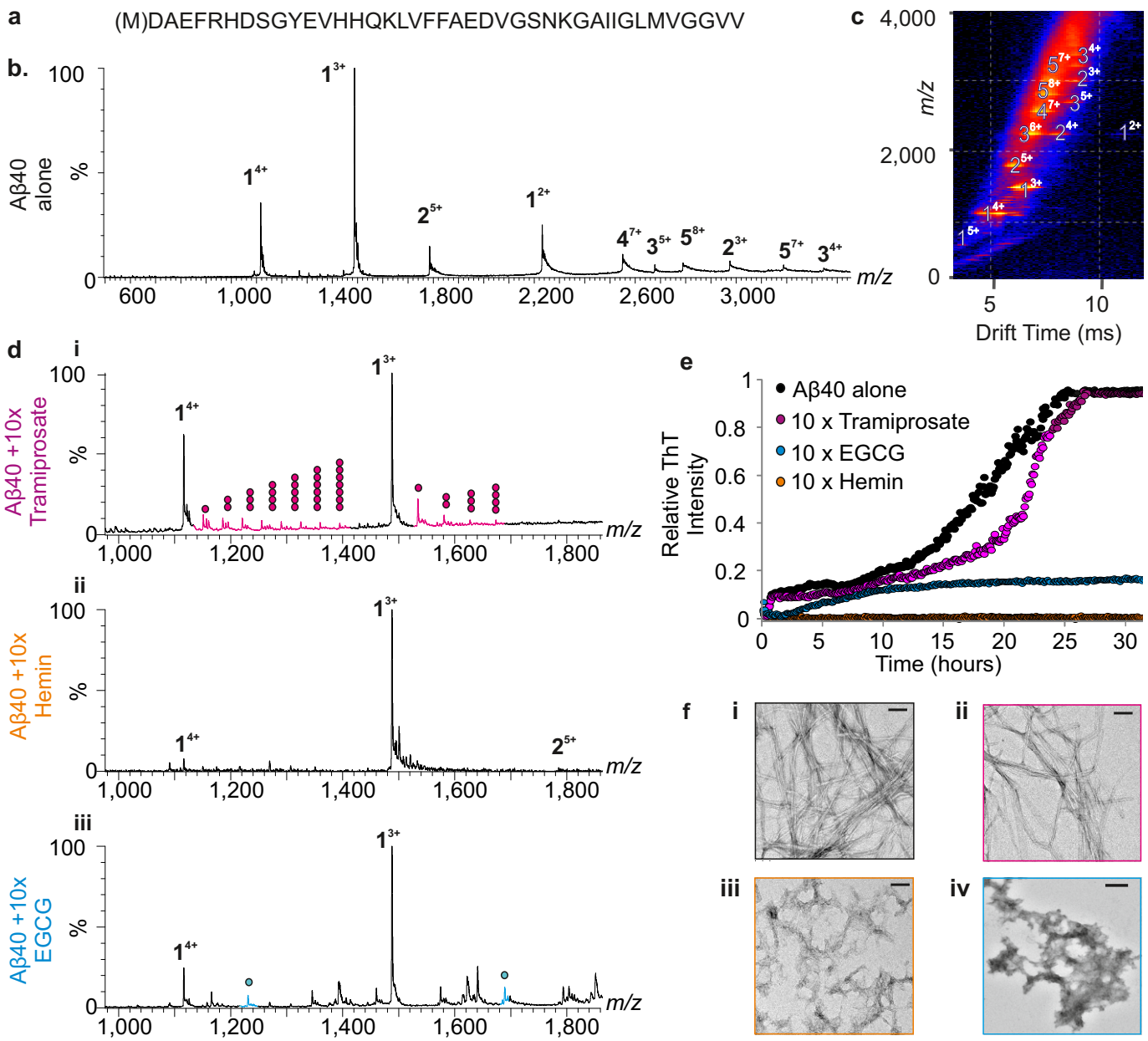
a
(M)DAEFRHDSGYEVHHQKLVFFAEDVGSNKGAIIGLMVGGVV
b.
Aβ40 alone
%
m/z
c
m/z
Drift Time (ms)
d
i
Aβ40 +10x Tramiprosate
ii
Aβ40 +10x Hemin
iii
Aβ40 +10x EGCG
e
Aβ40 alone
10 x Tramiprosate
10 x EGCG
10 x Hemin
Relative ThT Intensity
Time (hours)
f
i
ii
iii
iv